MINERALOGICAL MAGAZINE, DECEMBER 1986, VOL. 50, PP. 641-51

Evolution of the miscibility gap between muscovite and biotite solid solutions with increasing lithium content: an experimental study in the system K_2O–Li_2O–MgO–FeO–Al_2O_3–SiO_2–H_2O–HF at 600 °C, 2 kbar P_{H_2O}: comparison with natural lithium micas

GILLES MONIER

Laboratoire de Pétrologie, Université d'Orléans, 45046 Orléans Cedex, France

AND

JEAN-LOUIS ROBERT

Centre de Recherche sur la Synthèse et la Chimie des Minéraux, G.I.S. C.N.R.S.-B.R.G.M., 1A rue de la Férollerie, 45071 Orléans Cedex 2, France

ABSTRACT. This paper presents the results of an experimental study of the miscibility gap between trioctahedral and dioctahedral micas in the system K_2O–Li_2O–MgO–FeO–Al_2O_3–SiO_2–H_2O–HF at 600 °C, under 2 kbar P_{H_2O}. The existence of this miscibility gap is known from previous experimental studies. The gap is large in the lithium-free system; its width reduces progressively with increasing Li content; for sufficient Li contents (Li > 0.6 atom per formula unit, based on 11 oxygens), a single Li-mica phase is obtained, intermediate between trioctahedral and dioctahedral micas. Any bulk composition located inside the miscibility gap gives an assemblage of two micas, one of the biotite-type and one of the muscovite-type. All the compositions located outside the gap, and, in particular, those belonging to the joins phlogopite–trilithionite and muscovite–zinnwaldite (or its magnesian equivalent) give a single mica phase, provided that the fluorine content is sufficient. The ratio Li/F ≈ 1 is a convenient suitable value. The types of micas and the evolutions of their compositions are well characterized by their interplanar distance d_{060}. These experimental results allow the interpretation of most compositions of naturally occurring lithium micas, in the range $0 \leqslant Li \leqslant 1$ a./f.u. Natural micas of biotite-type and muscovite-type are located on both sides of the miscibility gap and their compositions get closer with increasing Li content.

KEYWORDS: biotite, muscovite, lithium mica, zinnwaldite, lepidolite, crystal-chemistry, experimental mineralogy, leucogranite.

© *Copyright the Mineralogical Society*

LITHIUM MICAS have been the subject of many experimental studies. These relate to the extent of solid solutions and to the stability of micas in the system polylithionite $[K(Li_2Al)Si_4O_{10}F_2]$–trilithionite $[K(Al_{1.5}Li_{1.5})(Si_3Al)O_{10}(OH,F)_2]$–muscovite $[K(Al_2\square)(Si_3Al)O_{10}(OH)_2]$, (Munoz, 1968, 1971); in the series siderophyllite $[K(Fe^{2+}_2Al)(Si_2Al_2)O_{10}(OH,F)_2]$–polythionite (Rieder, 1971); on the lines joining phlogopite $[KMg_3(Si_3Al)O_{10}(OH)_2]$ to each one of the three theoretical hydroxyl lepidolitic end members polylithionite, trilithionite and taeniolite $[K(Mg_2Li)Si_4O_{10}(OH)_2]$ (Robert and Volfinger, 1979); and on the join tetrasilicic magnesium mica $[KMg_{2.5}Si_4O_{10}(OH)_2]$–taeniolite (Robert, 1981).

Available experimental data are not sufficient to understand the compositions of most natural lithium micas and specially the compositions of iron–lithium micas having a Li content in the range 0–1 atom per formula unit, based on 11 oxygens; these micas are ferrous, aluminous, Li-bearing and have a variable proportion of vacant octahedral sites. Most of them are very complex and cannot be described as binary solid solutions. The composition of their tetrahedral layer is frequently close to Si_3Al.

This paper deals with the extent of the solid solution fields of lithium micas, principally those

with $0 < Li \leqslant 1$ a./f.u., based on 11 oxygens, having a constant composition of the tetrahedral layer (Si_3Al), in the system K_2O-Li_2O-Mg(Fe)O-Al_2O_3-SiO_2-H_2O-HF. This amounts to an exploration of the miscibility gap between dioctahedral and trioctahedral micas (Robert, 1976, 1981; Monier and Robert, 1986*a*), in the presence of lithium and fluorine. One knows, in effect, that no lepidolitic end member (polylithionite, trilithionite, taeniolite) is stable in the F-free system, whereas the fluorine end members are stable, and that a rough correlation exists between Li and F in natural micas (Foster, 1960; Rieder *et al.* 1970). Most lithium micas occur in pegmatites and in unusual differentiated facies of two mica granites. The *T*,*P* conditions 600 °C, 2 kbar are reasonable approximations of their crystallization environment and have been chosen for the experimental approach presented in this paper.

Experimental method, graphic representation, starting compositions

The experimental method used for the present work is identical to that described in previous papers dealing with similar systems (Robert, 1976; Robert and Volfinger, 1979; Monier and Robert, 1986*a*). The starting products were gels prepared according to the usual gelling method of Hamilton and Henderson (1968). Fluorine-bearing starting compositions were prepared by mixing a gel of appropriate composition, KF and $AlF_3 \cdot 3H_2O$.

The runs have been performed in gold tubes sealed by arc welding and placed in cold-seal pressure vessels. The ratio water/dry gel was kept constant, equal to 15 wt. %. The minimum run duration was 12 days and the temperature and pressure were maintained in the ranges 600 ± 5 °C, 2 kbar $\pm$ 50 bars for all runs. The identification and the characterization of run products were done by optical and scanning electron microscopies, X-ray diffraction and infra-red spectrometry. Infra-red data will be given and discussed in a forthcoming paper.

The lattice spacing d_{060}, which is very sensitive to compositional variations, has been measured for most synthetic micas, using Si as an internal standard and Cu-$K\alpha$ radiation ($\lambda = 1.5418$ Å).

The positions of the mica end members are plotted (fig. 1*a*) in a tetrahedron (Fe^{2+},Mg)-Li-Al-Si (atomic proportions). The basal plane, (Fe^{2+},Mg)-Al-Si contains the Li-free micas: phlogopite (Phl) (or annite, Ann) solid solutions, muscovite (Mu) solid solutions (see Robert, 1976, 1981; Monier and Robert, 1986*a*), and the tetrasilicic magnesium (or iron) mica, $KM^{2+}_{2.5}Si_4O_{10}(OH,F)_2$ (MTM). The Li-bearing end members are located in planes (cross-sections of the tetrahedron) parallel to the base (Fe^{2+},Mg)-Al-Si (fig. 1*a*). For Li = 1 atom per formula unit, two end members exist: taeniolite (Taen) $K(Mg_2Li)Si_4O_{10}(OH,F)_2$ and zinnwaldite (Zinn) $K(AlM^{2+}Li)(Si_3Al)O_{10}(OH,F)_2$; Li = 1.5 a./f.u. corresponds to trilithionite (Tril) $K(Al_{1.5}Li_{1.5})(Si_3Al)O_{10}(OH,F)_2$ and Li = 2 a./f.u. corresponds to polylithionite (Poly) $K(Li_2Al)Si_4O_{10}F_2$.

The starting compositions are indicated in a different and more classical representation, the plane M^{2+}-Li-Al (fig. 1*b*); Al includes Al^{IV} and Al^{VI}. In fig. 1*b*, four joins should be noted; they concern micas having the constant composition Si_3Al in the tetrahedral layer. These joins are: muscovite-trilithionite, muscovite-zinnwaldite, muscovite-phlogopite (or annite) and trilithionite-phlogopite (or annite).

Note about the name zinnwaldite. The mica corresponding to the structural formula $K(AlFe^{2+}Li)(Si_3Al)O_{10}(OH,F)_2$ is noteworthy because it is on the crossing of several important joins: the join annite-trilithionite ($Ann_{1/3}$ $Tril_{2/3}$), the join polylithionite-siderophyllite (Sid) $K(Fe^{2+}_2Al)(Si_2Al_2)O_{10}(OH,F)_2$ (zinnwaldite corresponds to $Poly_{50}Sid_{50}$; Rieder, 1971). In addition, it is the pole of the series muscovite-zinnwaldite and the pole of another, unexplored join, taeniolite-zinnwaldite. For these reasons, we suggest that the name zinnwaldite is restricted to this particular end member. Usually, in the literature, the name zinnwaldite is used to designate complex solid solutions around this point (Deer *et al.*, 1962; Bailey, 1984). The magnesian equivalent is not known in nature and we use the term magnesian zinnwaldite (MZ) to name it below.

Experimental results

We examine successively the results obtained from starting compositions belonging to the series phlogopite-trilithionite, to the series muscovite-zinnwaldite and muscovite-MZ and finally, to the two sections: zinnwaldite-A and B-C (fig. 1*b*). Data concerning solid solutions between Li-free dioctahedral and trioctahedral micas, i.e. the basal line M^{2+}-Al of the triangle M^{2+}-Li-Al (fig. 1*b*) are not developed here; they are taken from Monier and Robert (1986*a*) for muscovite solid solutions and from Robert (1976, 1981) for phlogopite solid solutions. Data on solid solutions between annite and muscovite are taken from a forthcoming paper on Li-free ferroaluminous biotites (Robert and Monier, in prep.). We summarize briefly the results obtained at 600 °C, 2 kbar on the joins phlogopite-muscovite and annite-muscovite. In muscovite solid solutions, the most magnesian mica on the

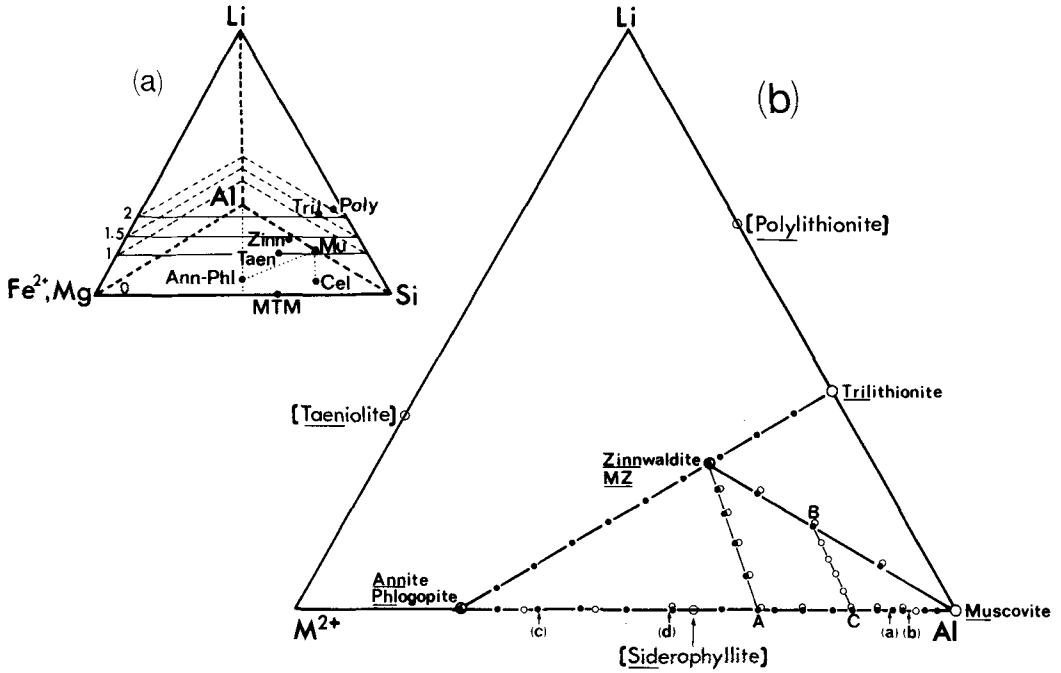

FIG. 1. (*a*) Positions of mica end members in the tetrahedron (Fe^{2+}-Mg)-Li-Al-Si. The planes 0, 1, 1.5, 2 contain, respectively, Li-free micas (Phl, Ann, Mu, Cel, MTM), micas with 1 Li a./f.u. (Taen, Zinn), 1.5 Li a./f.u. (Tril) and 2 Li a./f.u. (Poly). (*b*) Positions of mica end members having $Si^{IV}/Al^{IV} = 3$ and starting experimental compositions in the diagram M^{2+}-Li-Al. Along Zinn (or MZ)-A, Fe^{2+} (or Mg^{2+}) is constant and equal to 1 a./f.u.; along B-C, Fe^{2+} is constant and equal to 0.5 a./f.u. Square brackets indicate mica end members having a tetrahedral composition different from Si_3Al. (o) ferrous compositions; (●) magnesian compositions.

join muscovite-phlogopite has the formula:$K(Al_{1.8}Mg_{0.3}\square_{0.9})(Si_3Al)O_{10}(OH)_2$ (point (a), fig. 1*b*) and the most ferrous mica on the join muscovite-annite has the formula: $K(Al_{1.85}Fe^{2+}_{0.22}\square_{0.93})(Si_3Al)O_{10}(OH)_2$ (point (b), fig. 1*b*) (Monier and Robert, 1986*a*). In the biotites, the most aluminous mica has the formula: $K(Al_{0.4}Mg_{2.4}\square_{0.2})(Si_3Al)O_{10}(OH)_2$ (point (c), fig. 1*b*), in the magnesian system (Robert, 1976, 1981) and the formula: $K(AlFe^{2+}_{1.5}\square_{0.5})(Si_3Al)O_{10}(OH)_2$ (point (d), fig. 1*b*) in the ferrous system (Robert and Monier, in prep.).

The join phlogopite-trilithionite. From the phlogopite composition $KMg_3(Si_3Al)O_{10}(OH,F)_2$, the substitutional mechanism $2Mg^{VI} \rightleftharpoons Al^{VI}, Li^{VI}$ leads to trilithionite. The extent of solid solution from OH-phlogopite towards the theoretical OH-trilithionite end member has formed the aim of a detailed experimental study, from 400 to 900 °C, under 2 kbar P_{H_2O} (Robert and Volfinger, 1979). At no temperature does the composition of the theoretical OH-trilithionite produce a mica phase; at 600 °C it gives the assemblage α-eucryptite (α-$LiAlSiO_4$) + kalsilite + leucite. There is some solid solution between phlogopite and trilithionite in this F-free system which is important at low temperature (the most Li-rich mica on this join has the composition $Phl_{20}Tril_{80}$ at 400 °C). Solid solution decreases drastically with increasing temperature. At 600 °C, the temperature of interest in the present case, the most Li-rich mica on this join has the composition $Phl_{55}Tril_{45}$, beyond this limit, towards the theoretical OH-trilithionite end member, the assemblage mica + α-eucryptite + kalsilite + leucite is obtained.

By contrast, Munoz (1968) has proved the stability of the F-trilithionite end member between 400 and 670 °C, under the same water pressure, $P_{H_2O} = 2$ kbar. Therefore, we have resumed the study of the join phlogopite-trilithionite at 10 mole % intervals between OH-phlogopite and F-trilithionite and from the composition OH-$Phl_{1/3}$ F-$Tril_{2/3}$ (mica MZ); the results are given in Table I.

All the compositions investigated give a single mica phase on this join. The interplanar distance d_{060} decreases regularly from OH-phlogopite to F-trilithionite; the calculated regression line on the

Table I. Series OH-Phlogopite - F-Trilithionite ; 600°C,2 kbar

Condensed starting material	Phase assemblage	d_{060} (Å) Mica
$Phl_{100}Tril_0$; F_0	Mica	1.5350
$Phl_{90}Tril_{10}$; $F_{0.2}$	Mica	1.5351
$Phl_{80}Tril_{20}$; $F_{0.4}$	Mica	1.5308
$Phl_{70}Tril_{30}$; $F_{0.6}$	Mica	1.5264
$Phl_{60}Tril_{40}$; $F_{0.8}$	Mica	1.5231
$Phl_{50}Tril_{50}$; $F_{1.0}$	Mica, (α-eucryptite)	1.5203
$Phl_{40}Tril_{60}$; $F_{1.2}$	Mica, (α-eucryptite)	1.5166
$Phl_{1/3}Tril_{2/3}$; $F_{1.33}$(MZ)	Mica, (α-eucryptite)	1.5150
$Phl_{30}Tril_{70}$; $F_{1.4}$	Mica	1.5137
$Phl_{20}Tril_{80}$; $F_{1.6}$	Mica, (α-eucryptite)	1.5107
$Phl_{10}Tril_{90}$; $F_{1.8}$	Mica	1.5056
Phl_0Tril_{100} ; $F_{2.0}$	Mica	1.5017

Notes on Tables I-IV

The tables show principal compositions used in the determination of the extent of mica solid solutions along the joins OH-phlogopite - F-trilithionite (Table I), muscovite - zinnwaldite and mica MZ (Table II), and along the cross-sections zinnwaldite - mica A (Fe^{2+}), mica MZ - mica A (Mg), (Table III) and mica B (Fe^{2+}) - mica C (Fe^{2+}) (Table IV). Measured d_{060}(Å) of mica solid solutions.

Condensed starting products are given in terms of percentages of end members, F contents are in atoms per formula unit (a./f.u.) on the basis of 11 oxygens.

Mica: single phase mica solid solution; 2 Micas: two-mica solid solutions.

Average Δd value is 0.0003 Å when a single mica is present in the final product, and often greater in the two-mica assemblages. When two d_{060} values are given, the first is the value for the more trioctahedral phase. n.d. = not determined.

join OH-Phl-F-Tril is: d_{060} (Å) $= 1.5368 - 1.311 \cdot 10^{-6}X$ ($r = 0.997$), with X, the Li content of the mica, in ppm; this equation is similar to that obtained by Robert and Volfinger (1979) for the partial solid solution phlogopite-trilithionite, in the F-free system:

$$d_{060}\ (\text{Å}) = 1.535 - 1.235 \cdot 10^{-6}X.$$

From starting compositions lying between $OH\text{-}Phl_{50}F\text{-}Tril_{50}$ and $OH\text{-}Phl_{30}F\text{-}Tril_{70}$, traces of α-eucryptite appear occasionally in some run products. This accessory phase is the only one that has been observed on the join investigated; it cannot represent more than about 2% of the run product.

The difference between the extents of solid solution between phlogopite and trilithionite in the F-free and in the F-bearing systems is considerable and provides an additional example of the necessary coupling between Li and F for high Li contents, in substitutions leading to lepidolitic end members. This coupling is systematically observed in natural micas (Foster, 1960; Rieder *et al.*, 1970) as well as in experimental systems (Munoz, 1968, 1971; Robert and Volfinger, 1979); it provides a satisfactory explanation to the presence of anhydrous (and F-free) lithium aluminosilicates such as spodumene ($LiAlSi_2O_6$) and petalite ($LiAlSi_4O_{10}$) in pegmatites with very high Li/F ratio, instead of lepidolites (Černý and Burt, 1984).

The join muscovite-zinnwaldite (or mica MZ). In the system K_2O-$M^{2+}O$-Al_2O_3-SiO_2-H_2O, muscovite compositions are given by the general structural formula $K(Al_{2-x-\frac{2}{3}y}M^{2+}_{x+y}\square_{\frac{y}{3}})(Si_{3+x}Al_{1-x})O_{10}(OH)_2$, with x and y, the respective amounts of the phengitic substitution $Al^{VI},Al^{IV} \rightleftharpoons Mg^{VI},Si^{IV}$ and of the biotitic substitution $\frac{2}{3}Al^{VI},\frac{1}{3}\square^{VI} \rightleftharpoons Mg^{VI}$ (Monier and Robert, 1986*a*). Besides the series muscovite-trilithionite and muscovite-polylithionite studied experimentally by Munoz (1968), the fixation of Li in the octahedral layer of muscovite can be achieved according to the symbolic equation: $Al^{VI},\square^{VI} \overset{z}{\rightleftharpoons} (M^{2+})^{VI},Li^{VI}$ which leaves the tetrahedral layer unchanged and modifies the pure dioctahedral character of muscovite; z being the amount of this substitution, the formula of the series of lithium micas generated from the muscovite end member is $K(Al_{2-z}M^{2+}_zLi_z\square_{1-z})(Si_3Al)O_{10}(OH)_2$; muscovite corresponds to $z = 0$ and the zinnwaldite ($M^{2+} = Fe^{2+}$) and mica MZ ($M^{2+} = Mg^{2+}$) end members correspond to $z = 1$.

These series have been investigated experimentally in both ferrous and magnesian systems, with $z = 0, 0.25, 0.5, 0.75$ and 1 in the starting gel. Owing to the previously discussed required coupling between Li and F, the F content of the starting products has been increased at the same time as the Li content, up to a composition of the synthetic mica having OH_1F_1 atoms per formula unit, based on 11 oxygens, for $z = 1$, in the ferrous system, and to $OH_{0.67}F_{1.33}$ a./f.u. for $z = 1$, in the magnesian system. The experimental results on these series are in Table II. All the compositions investigated produce a unique mica phase, in the ferrous and in the magnesian systems, except for compositions

Table II. Series Muscovite-Zinnwaldite and Muscovite-MZ ; 600°C, 2 kbar

Condensed starting material	Phase assemblage	d_{060} (Å) Mica
Mu-Zinn		
$Mu_{100}Zinn_0$; F_0	Mica	1.4992
$Mu_{75}Zinn_{25}$; $F_{0.5}$	Mica	1.5040
$Mu_{50}Zinn_{50}$; $F_{1.0}$	Mica	1.5116
$Mu_{25}Zinn_{75}$; $F_{1.0}$	Mica	1.5200
Mu_0Zinn_{100} ; $F_{1.0}$	Mica, β-spodumene	1.5301
Mu-MZ		
$Mu_{75}MZ_{25}$; $F_{0.33}$	Mica	1.5015
$Mu_{50}MZ_{50}$; $F_{0.66}$	Mica	1.5045
$Mu_{25}MZ_{75}$; $F_{1.0}$	Mica	1.5110
Mu_0MZ_{100} ; $F_{1.33}$	Mica, (α-eucryptite)	1.5150

having $z = 1$. These give an assemblage of mica with traces of a lithium aluminum silicate, identified as α-eucryptite (α-$LiAlSiO_4$) from the magnesian end-member bulk composition and as β-spodumene (β-$LiAlSi_2O_6$) from the ferrous one; β-spodumene is a little more abundant in the two-phase assemblage obtained from the zinnwaldite composition (maximum 3-4%) than α-eucryptite in the product yielded from the MZ composition.

Fig. 2*a* shows the progressive increase of the interplanar distance d_{060} in the series muscovite-zinnwaldite and muscovite-MZ. In fig. 2*a* the value of d_{060} given by Rieder (1971) for a zinnwaldite synthesized in similar *T,P* conditions, *without accessory phase*, is plotted; this value agrees much better with the d_{060} of neighbouring micas of the series muscovite-zinnwaldite (fig. 2*a*) and zinnwaldite-A, see below (fig. 2*b*), than the value measured on our synthetic zinnwaldite sample. Hence, the presence of some β-spodumene in our run products indicates that we have not reached the true zinnwaldite end member from the starting composition having $z = 1$, but a slightly less lithian and more ferrous mica. From available data, we can propose an explanation to this difference. The fluorine content of MZ starting composition is 1.33 F a./f.u. based on 11 oxygens, i.e. F/Li = 1.33; this starting composition gives only traces of α-eucryptite accompanying the major mica phase. In the zinnwaldite (Fe^{2+}) gel, the initial ratio used here is F/Li = 1 and the composition gives more important amounts of the accessory phase, β-spodumene. Rieder (1971) succeeded in synthesizing this zinnwaldite end member, free of accessory phase, from a starting composition having the same ratio Li/F = 1, but by using the buffer calcite-fluorite-graphite (CFG) which is a further source of fluorine. Thus, it seems that the presence or the absence of accessory lithium aluminum silicates in the final product depends on the bulk Li/F ratio; for high Li/F ratio, some lithium cannot enter the mica structure and forms these anhydrous, and F-free, lithium aluminum silicates.

The main conclusion of these studies is the existence, under the experimental conditions used, of a continuous solid solution between muscovite and zinnwaldite and between muscovite and MZ. This provides therefore the second example of a complete solid solution between dioctahedral and trioctahedral micas; the other is the series muscovite-trilithionite, although a doubt remains about the existence of a narrow two-mica field around the composition muscovite 60%-trilithionite 40% (Munoz, 1968).

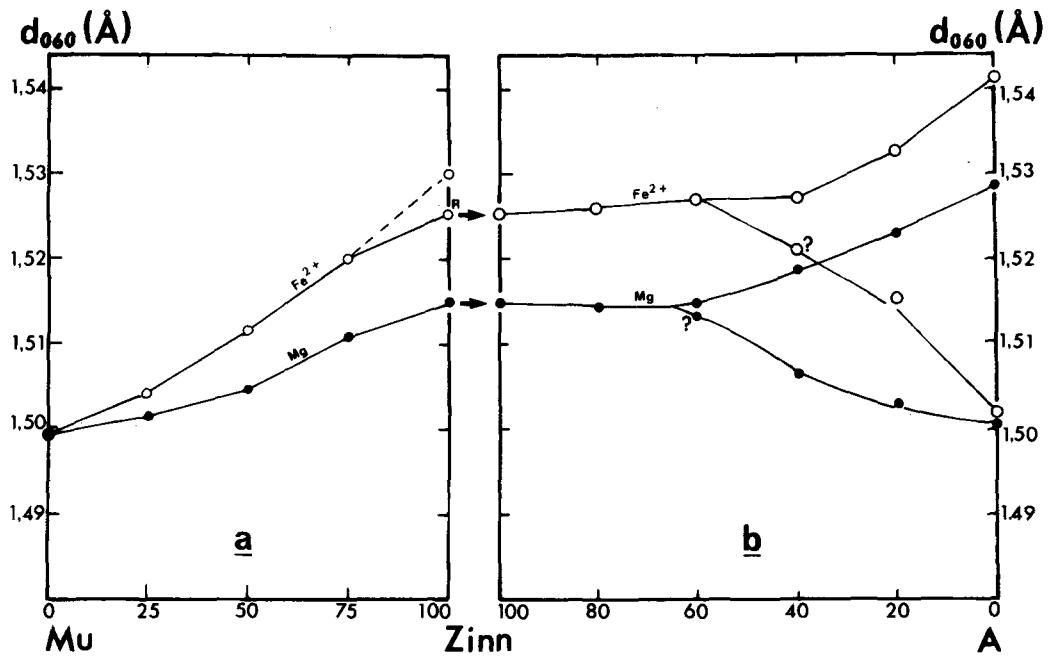

FIG. 2. Variations of d_{060} (Å): (*a*) in the micas of the series muscovite-zinnwaldite (Fe^{2+}) and muscovite-MZ (Mg^{2+}); (*b*) in the micas of the series zinnwaldite-A (Fe^{2+}) and MZ-A (Mg^{2+}). (o) ferrous compositions; (●) magnesian compositions; (o^R) zinnwaldite from Rieder (1971).

Study of compositions located inside the triangle annite (or phlogopite)–zinnwaldite (or MZ)–muscovite: sections Zinn–A and B–C (fig. 1b)

Two sections have been investigated. The first section, chosen so as to keep a constant Fe or Mg content, $M^{2+} = 1$ a./f.u., is between zinnwaldite (Zinn) or its magnesian equivalent (MZ) and a lithium-free mica A: $K(Al_{1.33}M^{2+}\square_{0.67})(Si_3Al)O_{10}(OH,F)_2$; the second section is between the starting composition B: $K(Al_{1.5}M^{2+}_{0.5}Li_{0.5}\square_{0.5})(Si_3Al)O_{10}(OH,F)_2$ and the lithium-free mica C: $K(Al_{1.67}M^{2+}_{0.5}\square_{0.83})(Si_3Al)O_{10}(OH,F)_2$ and corresponds to another constant iron or magnesium content, $M^{2+} = 0.5$ a./f.u. Between these poles, the starting compositions are at 20 mole % intervals along the two sections. The section zinnwaldite–A has been studied in the magnesian system (MZ–A) and in the ferrous system (Zinn–A); the section B–C has been investigated in the ferrous system only. The results are given in Tables III and IV.

Table III. Series Zinnwaldite - A (Fe^{2+}) and MZ - A (Mg); 600°C, 2 kbar

Condensed starting material	Phase assemblage	d_{060}(Å) Micas
Zinn-A(Fe^{2+})		
$Zinn_{100}A_0$; $F_{1.0}$	Mica, β-spodumene	1.5301
$Zinn_{80}A_{20}$; $F_{1.0}$	Mica	1.5261
$Zinn_{60}A_{40}$; $F_{1.0}$	Mica	1.5271
$Zinn_{40}A_{60}$; $F_{1.0}$	2 Micas	1.5272, (1.5210)
$Zinn_{20}A_{80}$; $F_{1.0}$	2 Micas	1.5328, 1.5156
$Zinn_0A_{100}$; $F_{1.0}$	2 Micas	1.5412, 1.5016
MZ-A(Mg)		
$MZ_{100}A_0$; $F_{1.33}$	Mica, (α-eucryptite)	1.5150
$MZ_{80}A_{20}$; $F_{1.20}$	Mica	1.5146
$MZ_{60}A_{40}$; $F_{1.07}$	2 Micas	1.5150, n.d.
$MZ_{40}A_{60}$; $F_{0.93}$	2 Micas	1.5190, 1.5067
$MZ_{20}A_{80}$; $F_{0.80}$	2 Micas	1.5231, 1.5033
MZ_0A_{100} ; $F_{0.67}$	2 Micas	1.5288, 1.5006

Table IV. Series B (Fe^{2+}) - C(Fe^{2+}); 600°C, 2 kbar

Condensed starting material	Phase assemblage	d_{060}(Å) Micas
$B_{100}C_0$; $F_{1.0}$	Mica	1.5116
$B_{80}C_{20}$; $F_{1.0}$	2 Micas	n.d.
$B_{60}C_{40}$; $F_{1.0}$	2 Micas	n.d.
$B_{40}C_{60}$; $F_{1.0}$	2 Micas	n.d.
$B_{20}C_{80}$; $F_{1.0}$	2 Micas	n.d.
B_0C_{100} ; $F_{1.0}$	2 Micas	n.d.

On the section MZ–A, in the magnesian system, the compositions MZ_{100} and $MZ_{80}A_{20}$ give a single mica phase whose interplanar distance d_{060} is constant (fig. 2*b*). From $MZ_{60}A_{40}$ to A_{100}, two micas crystallize in equilibrium, one of trioctahedral-type (high d_{060}), the other one of dioctahedral-type (low d_{060}); as shown by the evolution of d_{060} (fig. 2*b*), the compositions of these two micas diverge with a maximum difference at point A. On the section Zinn–A, the results are closely related to those obtained on the section MZ–A, but the assemblage of two micas appears for a zinnwaldite end member content of the starting product slightly below 60 mole %. All the compositions located along the section B–C, except for point B itself, yielded an assemblage of two micas whose compositions diverge progressively from B to C, as did those along the sections Zinn–A and MZ–A.

Comprehensive view of experimental results

Our results enable us to draw the limits of the field of stable compositions in the systems studied, with Fe^{2+} as well as Mg^{2+} (fig. 3). In the two systems, there is a large miscibility gap between Li-free trioctahedral and dioctahedral micas. The salient feature is the reduction of the width of this gap with increasing Li content of the mica. From any bulk composition situated inside the gap, for example x in fig. 3, an assemblage of two micas is obtained, one is of biotite-type and the other one of muscovite-type, respectively x_1 and x_2 (fig. 3) if Li is evenly distributed amongst the two micas, or rather x'_1 and x'_2 since the analyses of naturally occurring couples of biotite and muscovite show that Li usually favours the biotite-type mica. With increasing bulk Li-content, the compositions of the two micas in equilibrium migrate towards one another along the two sides of the miscibility gap. During this migration, muscovites get a more pronounced trioctahedral character, and the trioctahedral character of ferrous lithium biotites becomes more accentuated ($\square^{VI}$ decreases, see fig. 3).

From compositions situated outside the gap, and especially from high Li bulk compositions, provided that the F content is sufficient, a single mica phase crystallizes. The minimum Li content permitting the crystallization of this unique mica phase is Li > 0.6 a./f.u.; such a mica is at one and the same time Fe (or Mg)-rich, Li-bearing, aluminous and may or may not be vacancy-rich; it is close to the zinnwaldite end member or to its magnesian equivalent.

Comparison with natural lithium micas

Foster (1960) distinguishes two transitional series between lithium-free and lithium micas:

(*a*) the 'lithium aluminum micas', solid solutions between muscovite, trilithionite and polylithionite, with no or few divalent cations in the octahedral

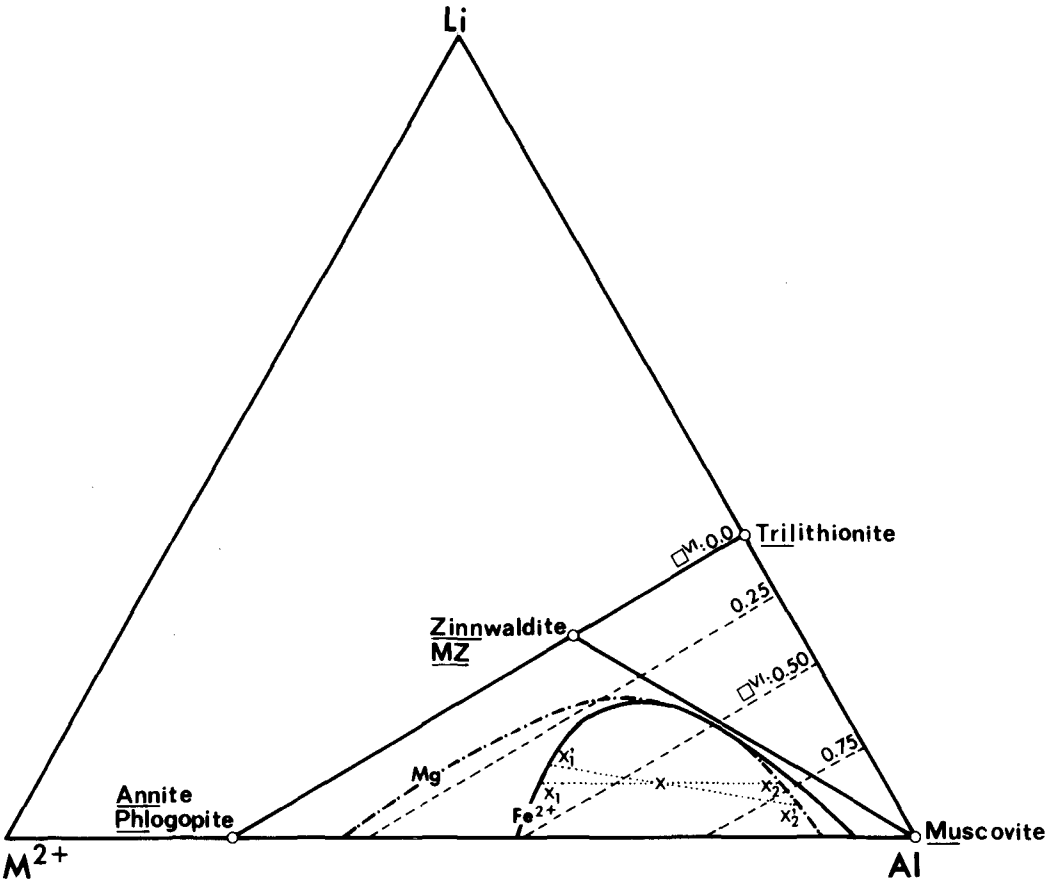

FIG. 3. Evolution of the miscibility gap between biotite and muscovite with increasing Li content in the ferrous (Fe^{2+}) and magnesian (Mg) systems. $\square^{VI}$ is the number of octahedral vacancies per formula unit.

sites. The compositions of this series lie along the Li-Al side of the triangular representation M^{2+}-Li-Al;

(*b*) the 'ferrous lithium micas', which represent a continuous series between ferrous biotites and lepidolites, this series is equivalent to the 'lithium-iron micas' (Rieder *et al.*, 1970; Rieder, 1971), i.e. the siderophyllite-polylithionite series.

To compare the experimental results presented in this paper with naturally occurring lithium micas, we have selected several series of Li-bearing micas from various origins; all are wet chemical analyses:

(*a*) the 'ferrous lithium micas' of Foster (1960);
(*b*) the 'lithium-iron micas' of Rieder *et al.* (1970);
(*c*) the 'zinnwaldites' of Heinrich (1967);
(*d*) the analyses, on separated minerals, of two sets of coexisting biotites and primary muscovites from granites from the French Massif Central; the first set comes from the Marche orientale massif (Gauthier, 1974) and the second one comes from the two-mica granite of the St Sylvestre massif (Monier, 1985).

These leucogranites exhibit important differentiation phenomena up to extremes highly enriched in Na, F, Li, Rb, ... (Ranchin, 1971; Gauthier, 1974; Friedrich, 1984). The crystal-chemical characters of their micas evolve with the differentiation of the host rock and lie in a wide range of compositions.

The compositions of these micas are plotted in a triangular diagram M^{2+}-Li-Al (fig. 4*a*, *b*, *c*) and in a diagram M^{2+}-Al-Si (fig. 5), similar to that previously used for the plot of Li-free dioctahedral and trioctahedral mica compositions (Robert, 1976; Monier and Robert, 1986*a*). Natural micas

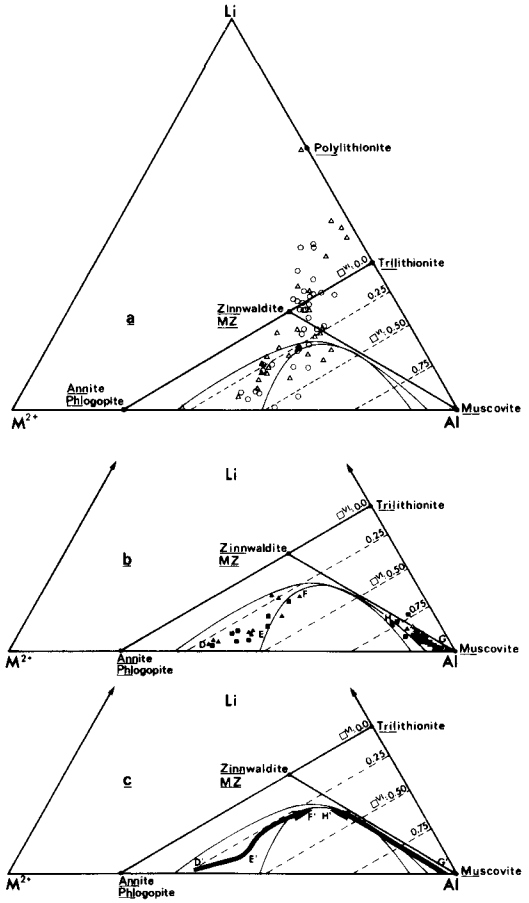

FIG. 4. Plot of compositions of various Li-bearing micas in the diagram M^{2+}–Li–Al. (*a*) (o) 'ferrous lithium micas' (Foster, 1960); (▲) 'lithium-iron micas' (Rieder *et al.*, 1970). (*b*) Coexisting biotites and muscovites from two-mica granites of the French Massif Central. (▲) Marche Orientale massif (Gauthier, 1974), (■) St Sylvestre massif, and zinnwaldites (☆) of Heinrich (1967). The hatched zone (lower right) shows the position of Li-free or Li-poor primary muscovites from two-mica granites (Monier and Robert, 1986*a*). (*c*) Heavy arrows represent the evolution of coexisting biotites and muscovites from two-mica granites of St Sylvestre; data from microprobe analyses, with Li estimated from F (see text and figs. 6 and 7). Significance of letters D, ..., H (fig. 4*b*) and D′, ..., H′ (fig. 4*c*) is detailed in the text.

have very complex compositions owing to additional substitutions involving principally Ti and Fe^{3+} in biotites and Ti,Fe^{3+} and $\square^{XII}$ (interlayer vacancy) in muscovites. An accurate plot of their compositions in diagrams such as M^{2+}–Li–Al or M^{2+}–Al–Si, requires taking into account these extra substitutions. The way to do this has been described and discussed in Robert and Maury (1979), Robert (1981) for biotites and in Monier and Robert (1986*a*) for muscovites.

Most lithium biotites from Foster (1960) and Rieder *et al.* (1970), with $0 < Li \lesssim 0.75$ a./f.u., have a composition of their tetrahedral layer close to Si_3Al (line annite (or phlogopite)–muscovite; fig. 4*a*); they lie near the left side of the stable composition domain determined experimentally in the ferrous system (fig. 4*a*). For $0.75 \lesssim Li \leqslant 1$ the compositions are closed to the zinnwaldite end member; for $Li > 1$, the micas become more and more siliceous and their compositions move away from the annite–muscovite line towards the polylithionite end member (Rieder *et al.*, 1970). The pronounced curvature in the evolution trend of these micas is striking (fig. 5). The study of micas with high Li contents, $Li > 1$, is beyond the scope of this paper.

The compositions of micas from leucogranites from the French Massif Central are plotted in figs. 4*b* and 5. These micas are characterized by a remarkably constant composition of their tetrahedral layer, Si_3Al, even more constant than Foster's and Rieder's micas, which places them along the annite–muscovite line. During the differentiation of the granitic massifs, biotites move away from the annite (phlogopite) end member and become more and more aluminous and octahedral vacancy-rich (D–E, figs. 4*b* and 5). In a first stage, the enrichment in Li is slight; it becomes important when the compositions meet the miscibility gap observed experimentally in the ferrous system (point E, figs. 4*b* and 5). From point E, the compositions evolve along the M^{2+}-rich side of the curve limiting this miscibility gap (E–F, figs. 4*b* and 5). The most vacancy-rich biotites are located at E; beyond this limit a further enrichment in Li produces a decrease in the proportion of octahedral vacancies in biotites. The discontinuity at point E in the trend DEF lies very close to the M^{2+}-rich side of the experimentally determined immiscibility gap for the Fe system. This shows that the experimental model system solvus is very close to the natural system.

Similarly, during the differentiation of the host rock, the white micas move away from the muscovite end member and have an increasingly trioctahedral character. Their compositions migrate along the Al-rich side of the miscibility gap (G–H, figs. 4*b* and 5) near the join muscovite–zinnwaldite.

The range of the variations, i.e. the enrichment in Li, F ... in these muscovites appears to be much more restricted ($Li \leqslant 0.30$, $Fe^{2+} \leqslant 0.29$) than in coexisting biotites, but this is due to a purely technical reason: electron microprobe analysis of muscovites from the most differentiated parts of the

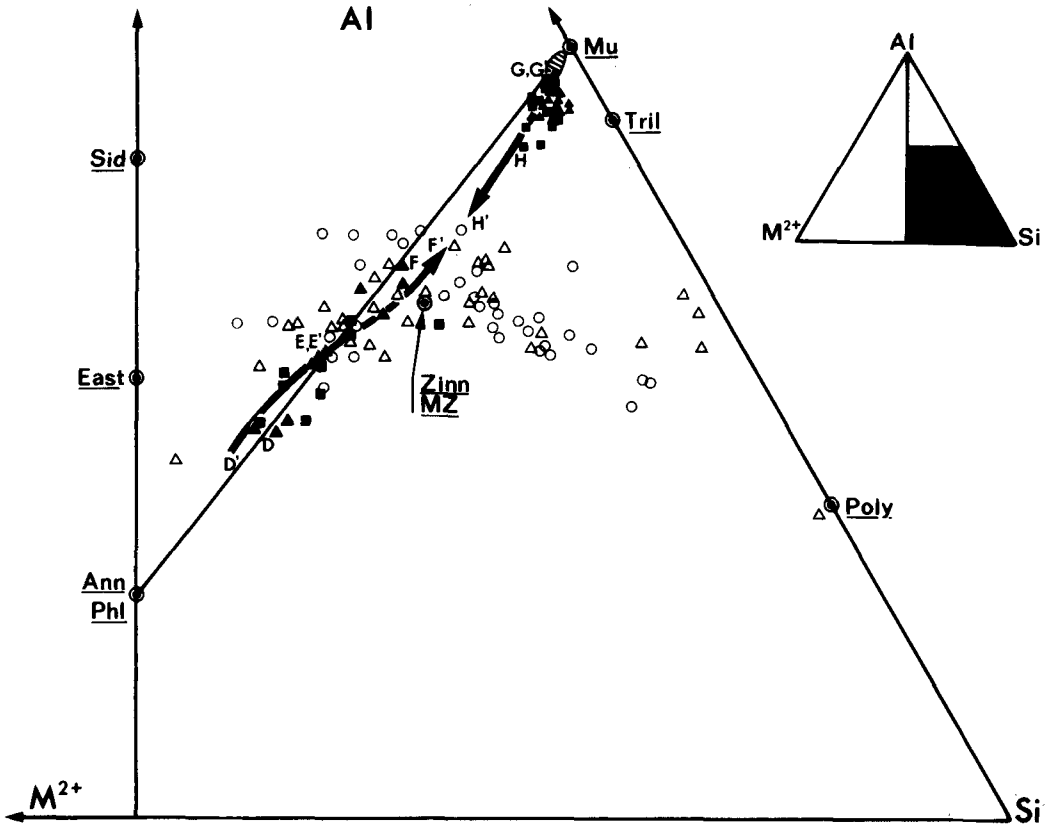

FIG. 5. Plot of compositions of 'ferrous lithium micas' (Foster, 1960), 'lithium–iron micas' (Rieder *et al.*, 1970) and of coexisting biotites and muscovites from two-mica granites of French Massif Central in the diagram M^{2+}–Al–Si. Symbols, shaded zone and heavy arrows as in fig. 4*a*, *b*, *c*.

granitic massifs shows significant zoning; only the external parts of muscovite crystals are strongly enriched in F, Fe^{2+} and most likely Li, whereas biotite crystals are homogeneous (Monier and Robert, 1986*b*). Therefore, since wet chemical analysis gives an average value, high lithium 'muscovites' cannot be identified. The analysis of these zoned micas needs point analysis methods suitable for light elements, such as ion probe or nuclear methods (Basutçu *et al.*, 1983).

Fig. 6 shows the variations of the sum Fe + Mg + (Mn) a./f.u. and of the F* content from more than 360 point electron microprobe analyses of coexisting biotites and muscovites from the leucogranitic massif of St Sylvestre. One notes a clear positive correlation (G'–H') between F and M^{2+} in muscovites (low M^{2+}) and a clear negative correlation in biotites (D'–E'–F'). The compositions of micas of the two families become closer with increasing fluorine content.

Owing to the impossibility of analysing of Li with the electron microprobe, any direct comparison with experimental results is problematic. In fig. 7 the Li_2O content of micas is plotted as a function of their F content (wt. %). Both Li_2O and F have been measured by wet chemical analysis on the separated micas from St Sylvestre massif plotted in figs. 4*b* and 5. A good positive correlation exists between Li_2O and F for both muscovite-type and biotite-type micas which permits estimation of the Li content of micas from their F content determined by electron microprobe analysis. Considering this correlation, the structural formulae of lithium micas could be calculated from microprobe analysis. Figs. 4*c* and 5 show the evolution of muscovites and biotites (heavy arrows) in M^{2+}–Li–Al and M^{2+}–Al–Si diagrams. The correspondence between these estimated lithium

* The fluorine content is given in weight percent. Because the analytical method does not allow the determination of H_2O^+, the calculation of X_F is impossible with accuracy.

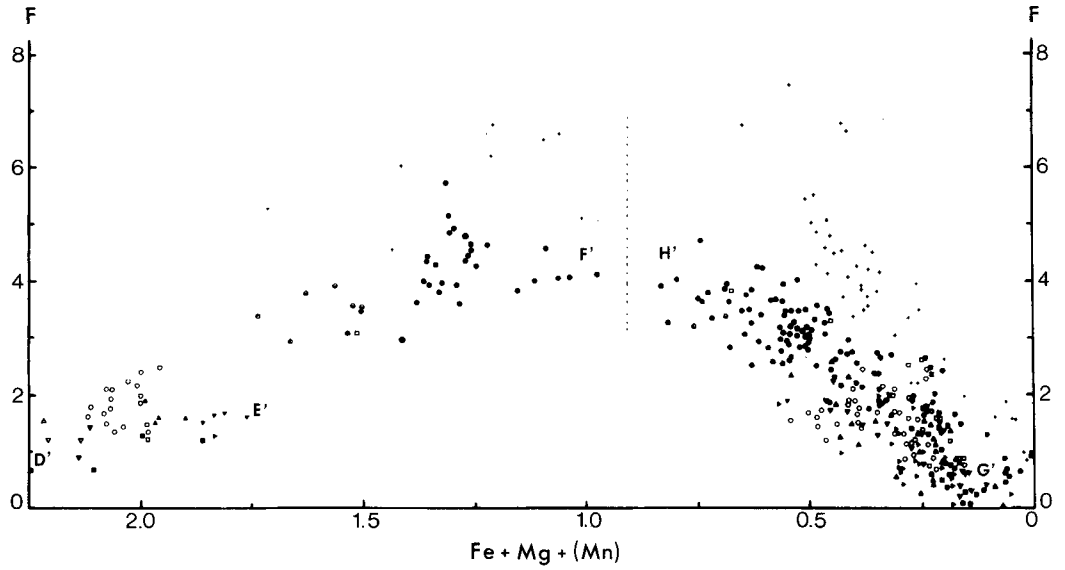

FIG. 6. Variation of the sum Fe+Mg+(Mn) a./f.u. and of the F content (weight percent) from electron microprobe analyses of coexisting biotites and muscovites from the two-mica granites of St Sylvestre massif. The dotted line separates 'muscovites' on the right from 'biotites' on the left.

contents and those measured by wet chemical analysis (figs. 4*b* and 5) is good and it is possible to consider that this treatment provides a suitable approximation.

From these data we have now a rather complete panoramic view of the behaviour of lithium micas, for $0 < Li \leqslant 1$.

The series of 'ferrous lithium micas' of Foster (1960) and the series of 'lithium-iron micas' of Rieder *et al.* (1970) represent, for $Li < 1$, the evolution of compositions of biotites having a high X_{Fe}, with increasing Li content, along the M^{2+}-rich side of the miscibility gap between trioctahedral and dioctahedral micas. The muscovites coexisting with these biotites migrate along the Al-rich side of the gap. This is identical to the experimental results: there is an equilibrium between two micas, one of the trioctahedral-type, the other of the dioctahedral-type, situated on the two sides of the miscibility gap. Their compositions become progressively closer with increasing bulk Li content. From high Li compositions, a unique mica crystallizes.

Compared to Foster's classification involving 'ferrous lithium micas' and 'aluminum lithium micas', this work shows a third transitional series between lithium-free and lithium micas, close to the join muscovite–zinnwaldite that could be named 'ferrous aluminum lithium micas'. The observation of compositions of natural lithium micas emphasizes its importance.

This work has an additional conclusion: the occurrence of micas belonging to the series of 'aluminum lithium micas' of Foster is limited to

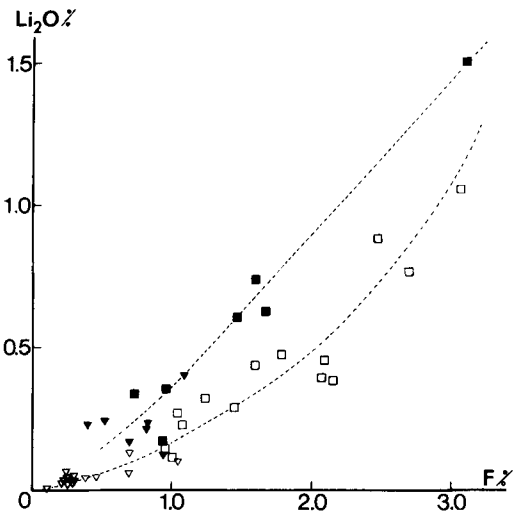

FIG. 7. Correlation F/Li_2O for separated biotites and muscovites from St Sylvestre massif (see fig. 4*b*) and from Li-poor two-mica granites of Millevaches massif (French Massif Central; Monier, 1980). (□, ■) St Sylvestre massif; (▽, ▼) Millevaches massif. White symbols are for muscovites, black symbols are for biotites.

crystallization environments depleted in Fe^{2+}, Mg^{2+} and Mn^{2+} (for example some pegmatites, greisens or some highly hololeucocratic granites) and they cannot coexist in equilibrium with ferromagnesian micas.

Acknowledgements. One of us (G.M.) is indebted to the Commissariat à l'Energie Atomique (C.E.A.-D.A.M.N.) for financial support.

REFERENCES

Bailey, S. W. (1984) In *The Micas* (S. W. Bailey, ed.) *Reviews in Mineralogy* **13.** Mineral soc. Am., 1–2.

Basutçu, M., Barrandon, J.-N., Volfinger, M., and Robert, J.-L. (1983) *Chem. Geol.* **40,** 353–9.

Černý, P., and Burt, D. M. (1984) In *The Micas* (S. W. Bailey, ed.) *Reviews in Mineralogy* **13.** Mineral Soc. Am., 257–97.

Deer, W. A., Howie, R. A., and Zussman, J. (1962) Rock Forming Minerals **3,** *Sheet Silicates.* Longmans, London.

Foster, M. D. (1960) *U.S. Geol. Surv. Prof. Paper* 354-E, 115–46.

Friedrich, M. (1984) *Géol. Géochim. Uranium,* Mém. Nancy, France, 5, 361 pp.

Gauthier, J.-C. (1974) *Sci. de la Terre,* **19,** 119–51.

Hamilton, D. L., and Henderson, C. M. B. (1968) *Mineral. Mag.* **36,** 832–8.

Heinrich, E. W. (1967) *Am. Mineral.* **52,** 1110–21.

Monier, G. (1980) Thèse de 3e cycle, Univ. Clermont II, France, 288 pp.

——(1985) Thèse d'Etat, Univ. Orléans, 299 pp.

——and Robert, J.-L. (1986*a*) *Mineral. Mag.* **50,** 257–66.

————(1986*b*) *Neues Jahrb. Mineral. Abh.* **153,** 147–61.

Munoz, J. L. (1968) *Am. Mineral.* **53,** 1490–512.

——(1971) Ibid. **56,** 2069–87.

Ranchin, G. (1971) *Sci. de la Terre,* Mém. 19, Nancy, France.

Rieder, M. (1971) *Am. Mineral.* **56,** 256–80.

——Huka, M., Kucerova, D., Minarik, L., Obermajer, J., and Povondra, P. (1970) *Contrib. Mineral. Petrol.* **27,** 131–158.

Robert, J.-L. (1976) *Chem. Geol.* **17,** 195–212.

——(1981) Thèse d'Etat, Univ. Paris XI, France, 206 pp.

——and Maury, R. C. (1979) *Contrib. Mineral. Petrol.* **68,** 117–23.

——and Volfinger, M. (1979) *Bull. Minéral.* **102,** 21–5.

[*Manuscript received 2 April 1985; revised 28 October 1985*]